Craig C. Smith
Department of Mechanical Engineering
Brigham Young University
Provo, UT 84602-4102, USA

Forrest L. Staffanson
Ogden Engineering Laboratory TRW
Strategic Systems Division

Basic Mechanical Interactions in Shaker Testing

Simple models representing a shaker and a test object are used to illustrate changes in test object response due to shaker dynamics and differences between the test and service environment. The degree of coupling is quantified in terms of ratios of the natural frequencies and the masses. Regions of overstress can depend on reproducing absolute rather than relative motion in a test. Shaker tests reprodusing output spectra observed in service, when shaker/fixture impedance is higher than the impedance in service, is shown to cause overtest at frequencies below natural frequencies of the service environment.

INTRODUCTION

For many years vibration shakers have been used for dynamic environmental testing of structures before they are put into service. Military and aerospace structures, where failures are especially expensive, are thoroughly tested before being cleared for use. Virtually all shaker testing is based upon the underlying assumption that dynamic (modal) properties of the test object are unchanged between service and testing. If the process of testing introduces significant changes in the dynamic properties, the test may become meaningless. Because attaching the test object to a shaker rather than to its service environment always introduces some changes, the important question is when these changes are *significant* and when they are insignificant.

We examine the energetic interactions between the test object and its environment to determine the degree to which the dynamic properties of the test object are altered by a change in its environment. The *impedances* at the locations (*ports*) where energy is exchanged between the object and its environment determine how much coupling occurs. Coupling is tantamount to changing the dynamic properties of the test article. Therefore, the impedances at these ports are the focal points of our attention in determining the significance of changes. If the impedances at all ports are unchanged, then the dynamic (modal) properties of the test object are unchanged. Because impedance is a function of frequency, it is only necessary (in an engineering sense) to require that the impedances remain unchanged over frequency ranges where significant energetic interaction is likely to occur. Any particular mode is relatively unaffected by changes in impedance at frequencies far removed from the natural frequency of the mode.

We note in passing that a mode of the test object far removed *spatially* from a port is also unaffected by changes in boundary conditions at the port. The test object in such a case could be redefined as a component part of the object mounted on a shaker, hav-

Received January 19 1996; Revised April 30 1997.
Shock and Vibration, Vol. 4, No. 4, pp. 269–280 (1997)
ISSN 1070-9622/97/$8.00 © 1997 IOS Press

ing its ports near the new test object with unchanged impedances. In general, heavily damped structures will allow boundary changes in a "far field" without creating significant local changes, because energy is dissipated before reaching the "near field" after reflection or emission at the far field. In general, however, changes at boundaries of lesser damped structures can cause significant changes at points far removed from the location of the changed boundary conditions.

New shakers of increasing capability are being placed into service (Bausch and Good, 1992, 1995; Chang and Frydman, 1990; Hershfield, 1995). Multiaxis shakers are being developed, and control systems are being designed to control multiple axes simultaneously to produce more realistic environmental testing. Sometimes the specifications for the controllers for these shakers include control over ranges that far exceed the range over which shaker dynamics are negligible. This raises some of the questions discussed in this article: over what ranges can the impedance between the shaker and test object be considered "similar" to that between the test object and its environment during service? Additionally, current considerations for revision of MIL-STD-810 and MIL-STD-331 raise issues of how carefully boundary conditions must be reproduced in testing to insure test validity. The possible advantages of using multiaxis shakers may be negated by the inability to control the boundary conditions.

The incorrect definition of boundary conditions has long been a concern to finite element modelers. The differences between finite element model predictions and actual tests can be improved by the identification of boundary conditions or joint parameters through measured frequency response functions (Yang and Park, 1993). Just as boundary condition variation significantly affects the validity of finite element models, it also affects the validity of hardware models used in shaker tests.

Recent studies (Scharton, 1990, 1991, 1993a) have focused upon limiting the forces at the excitation points in a structure to control overtest because large stresses typically occur in testing when the interface impedances are not the same during testing as during service. This approach has the potential of controlling the impedances to more closely resemble the service environment. If force limiting is necessary, however, it is obvious that the interface impedance changes are significant; thus, the dynamic properties of the test object have been significantly changed, as have the forces (stresses) in the test object. Force limiting potentially controls these stresses from getting too high (relative to in-service conditions) in one location (near the interface). But if the mode shapes have changed, critical stresses may occur at other locations or be reduced at in-service critical locations. Changing the impedance at an interface changes the natural frequencies of the system and moves the nodes and antinodes of the corresponding mode shapes. Thus, the test system is not dynamically the same as the system in service, and dynamic failures will not replicate in-service failures.

The following discussion, after introducing simple oscillator models that mention bond graphs and causality, illustrates and quantifies effects of coupling and differing boundary conditions between service and testing. Results are calculated for several combinations of infinite impedance or coupling on the shaker with infinite impedance or coupling in the service environment.

MODELS

To examine mechanical interactions, consider the following simple models. The three passive phenomena that exist in all mechanical structures are inertia, compliance, and dissipation. The simplest mechanical two-port element that contains all of these phenomena is the two-port oscillator illustrated in Fig. 1, where the three passive phenomena are indicated by m, k, and b. It may be called an oscillator because it will show natural oscillatory behavior if the damping is low enough, because it has both inertia and compliance that store kinetic and potential energy. It is a two-port oscillator because it can interact with its environment at two interfaces where power may be transferred between it and its environment. These interfaces are thus called power ports. Each port has a pair of power variables associated with it, one of the pair being a force and the other being a velocity. The product of the force transmitted at the interface and the velocity at the interface is power; thus, force and velocity are called power variables. Therefore f_a and v_a define the power at port a while f_b and v_b define the power at port b.

A bond graph provides a convenient means of assuring proper modeling, including causality (Karnopp and Rosenberg, 1975). Figure 2 is bond graph for the simple mechanical oscillator of Fig. 1. Power at ports a and b are considered positive when power flows into the oscillator at port a and out of the oscillator at port

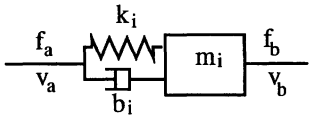

FIGURE 1 Simple mechanical two-port oscillator.

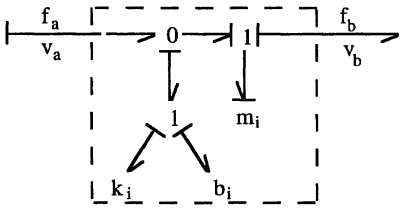

FIGURE 2 Bond graph for two-port oscillator.

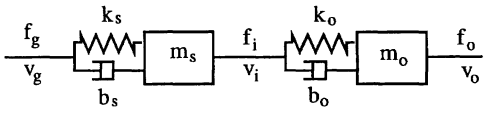

FIGURE 3 Two degree of freedom model.

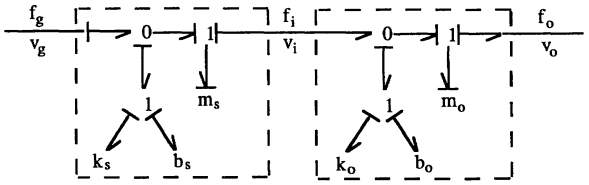

FIGURE 4 Two degree of freedom bond graph.

b, respectively. This positive power convention is denoted by the half arrowheads on the respective bonds. The causal stroke (line at one end of the bond perpendicular to the bond) at bond a denotes that v_a (flow or motion variable) will be considered an input to the oscillator. Thus, v_a is defined by the external environment that interacts with the oscillator through bond a, whereas f_a (effort variable) is an output defined by the oscillator dynamics. Similarly, the causal stroke on bond b indicates that f_b is considered an input to the oscillator while v_b is considered an output. Causality refers to the definition of inputs and outputs, because inputs *cause* outputs. Note that at each port at which the oscillator interacts with its environment, one and only one power variable can be an input to the oscillator whereas the other is an output from the oscillator. Of course, the input and output roles of these variables are reversed with respect to the external environment at each port.

The transfer functions relating the inputs and outputs for the simple oscillator in the given causal arrangement of Fig. 1 can be written as

$$\begin{Bmatrix} f_a \\ v_b \end{Bmatrix} = \begin{bmatrix} \dfrac{\beta_i}{\Delta_i} & \dfrac{m_i \beta_i s}{\Delta_i} \\ -\dfrac{s}{m_i \Delta_i} & \dfrac{\beta_i}{\Delta_i} \end{bmatrix} \begin{Bmatrix} f_b \\ v_a \end{Bmatrix}, \quad (1)$$

where $\beta_i = 2\zeta_i \omega_i s + \omega_i^2$, $\Delta_i = s^2 + \beta_i$ and while $\omega_i = \sqrt{k_i/m_i}$ and $\zeta_i = b_i/2\sqrt{k_i m_i}$.

Suppose that a structure that we wish to test on a shaker can be modeled within the frequency range of interest by this simple model. As described in detail in another article (Smith and Staffanson, 1996), the dynamic characteristics of a structure can be modeled in frequency regions by the mode(s) that dominate at those frequencies. Thus, the simple modal oscillator model will yield general results when properly applied.

Assume, for example, that in service the structure at port a is fixed, so that $v_a = 0$, and that the input excitation is a force applied at port b (perhaps acoustic excitation). The only input then is f_b. Assume further that because we cannot measure f_b in service, we instead measure the velocity v_b (or equivalently the acceleration at b). This measurement is typically represented by an autospectral density A_b of the acceleration at location b. Let us assume that the structure fails when the force f_a exceeds some level (stress at some point in the structure gets too large) and that the objective of the test is to produce with a shaker a force f_a^t that is statistically the same as f_a^s experienced in service.

Suppose in testing, instead of trying to duplicate the input f_b^s, we attach a shaker at port a and provide input v_a^t such that the resulting force f_a^t is statistically the same as f_a^s. As in a similar case discussed in a latter section, the desired result can be achieved if the relative velocity $(v_b - v_a)$ is statistically the same as that in service. Controlling the shaker such that the input v_a results in an autospectrum of $(v_b - v_a)$, which is the same as in service, will produce an autospectral density at port a the same as that in service. (Note $v_a = 0$ in service, so $[A_b + A_a - C_{ab} - C_{ba}]_{\text{test}} = [A_b]_{\text{service}}$, where A_i denotes the autospectrum at i and C_{ij} denotes the cross spectrum between i and j.) Thus, structural failure in testing would imply failure in service. Because there is not coupling with the environment in service or in testing, the dynamic properties (eigenvalues) of the structure are unchanged and proper excitation by the shaker can faithfully reproduce the dynamic response that would occur in service.

Now let us consider the more general case in which the dynamics of the supporting structure must be taken into account. A 2-degree of freedom model can be constructed by cascading two 1-degree of freedom two-port elements as shown in Figs. 3 and 4, where each of the elements interacts via a single bond i, with power variables f_i and v_i. The other ports will be labeled g and o with power variables (f_g, v_g) and (f_o, v_o), respectively. Note that the parameters of one oscillator are denoted by the subscript s (supporting structure in service or on the shaker); those of the other are denoted by the subscript o (test object).

Using Eq. (1) with appropriately permuted subscripts to represent both elements in Fig. 4, the transfer functions below are determined, relating the inputs to the 2-degree of freedom model to the outputs:

$$v_i = \frac{-\frac{s}{m_s}\beta_o}{\Delta_s\Delta_o + s^2\frac{m_o}{m_s}\beta_o} f_o + \frac{\beta_s\Delta_o}{\Delta_s\Delta_o + s^2\frac{m_o}{m_s}\beta_o} v_g, \tag{2}$$

$$f_i = \frac{\beta_o\Delta_s}{\Delta_s\Delta_o + s^2\frac{m_o}{m_s}\beta_o} f_o + \frac{sm_o\beta_o\beta_s}{\Delta_s\Delta_o + s^2\frac{m_o}{m_s}\beta_o} v_g, \tag{3}$$

$$v_o = \frac{-\frac{s}{m_o}(\Delta_s + \frac{m_o}{m_s}\beta_o)}{\Delta_s\Delta_o + s^2\frac{m_o}{m_s}\beta_o} f_o + \frac{\beta_o\beta_s}{\Delta_s\Delta_o + s^2\frac{m_o}{m_s}\beta_o} v_g. \tag{4}$$

Normalizing the terms by dividing all frequencies by the natural frequency ω_o, let $\bar{s} = s/\omega_o$, $\bar{\beta}_i = \beta_i/\omega_o^2$, and $\bar{\Delta}_i = \Delta_i/\omega_o^2$, the transfer functions in Eqs. (2)–(4) can be written in nondimensional form:

$$v_i = \frac{-\bar{s}M\bar{\beta}_o}{\bar{\Delta}_s\bar{\Delta}_o + \bar{s}^2M\bar{\beta}_o}\frac{f_o}{m_o\omega_o} + \frac{\bar{\beta}_s\bar{\Delta}_o}{\bar{\Delta}_s\bar{\Delta}_o + \bar{s}^2M\bar{\beta}_o} v_g, \tag{5}$$

$$\frac{f_i}{m_o\omega_o} = \frac{\bar{\beta}_o\bar{\Delta}_s}{\bar{\Delta}_s\bar{\Delta}_o + \bar{s}^2M\bar{\beta}_o}\frac{f_o}{m_o\omega_o} + \frac{\bar{s}\bar{\beta}_o\bar{\beta}_s}{\bar{\Delta}_s\bar{\Delta}_o + \bar{s}^2M\bar{\beta}_o} v_g, \tag{6}$$

$$v_o = \frac{-\bar{s}(\bar{\Delta}_s + M\bar{\beta}_o)}{\bar{\Delta}_s\bar{\Delta}_o + \bar{s}^2M\bar{\beta}_o}\frac{f_o}{m_o - \omega_o} + \frac{\bar{\beta}_o\bar{\beta}_s}{\bar{\Delta}_s\bar{\Delta}_o + \bar{s}^2M\bar{\beta}_o} v_g, \tag{7}$$

where

$$\bar{\beta}_o = 2\zeta_o\bar{s} + 1, \quad \bar{\Delta}_o = \bar{s}^2 + \bar{\beta}_o,$$
$$\bar{\beta}_s = 2\zeta_s\bar{\omega}_s\bar{s} + \bar{\omega}_s^2, \quad \bar{\Delta}_s = \bar{s}^2 + \bar{\beta}_s,$$

and

$$M = \frac{m_o}{m_s}, \quad \bar{\omega}_s = \frac{\omega_s}{\omega_o}.$$

To convert the above equations to the frequency domain, we substitute $s = j\omega$ so that $\bar{s} = j(\omega/\omega_o) = j\bar{\omega}$, where $\bar{\omega} = \omega/\omega_o$. Thus, the above equations become

$$\bar{v}_i = \frac{-j\bar{\omega}M\bar{\beta}_o}{\bar{\Delta}_s\bar{\Delta}_o - \bar{\omega}^2M\bar{\beta}_o} \bar{f}_o + \frac{\bar{\beta}_s\bar{\Delta}_o}{\bar{\Delta}_s\bar{\Delta}_o - \bar{\omega}^2M\bar{\beta}_o} \bar{v}_g, \tag{8}$$

$$\bar{f}_i = \frac{\bar{\beta}_o\bar{\Delta}_s}{\bar{\Delta}_s\bar{\Delta}_o - \bar{\omega}^2M\bar{\beta}_o} \bar{f}_o + \frac{j\bar{\omega}\bar{\beta}_o\bar{\beta}_s}{\bar{\Delta}_s\bar{\Delta}_o - \bar{\omega}^2M\bar{\beta}_o} \bar{v}_g, \tag{9}$$

$$\bar{v}_o = \frac{-j\bar{\omega}(\bar{\Delta}_s + M\bar{\beta}_o)}{\bar{\Delta}_s\bar{\Delta}_o - \bar{\omega}^2M\bar{\beta}_o} \bar{f}_o + \frac{\bar{\beta}_o\bar{\beta}_s}{\bar{\Delta}_s\bar{\Delta}_o - \bar{\omega}^2M\bar{\beta}_o} \bar{v}_g. \tag{10}$$

FREQUENCY UNCOUPLING OF MODES

One of the important tenets of shaker testing is the idea of frequency uncoupling. That is, as modal dynamics become separated in frequency, they become uncoupled. Thus, excitation in one frequency band excites modes (natural frequencies) within that band, but not those modes outside that band. We thus *shape* the excitation according to frequency to excite the modes of interest. Here we will use the same concept to determine the effect of the coupling between the two oscillators above as a function of the ratio of their natural frequencies. We will then examine the effects of this coupling (or uncoupling) in practical shaker situations.

To locate the resonances of the shaker test object system, we look at the roots of the denominator of the transfer functions [Eqs. (5)–(7)]. Letting

$$\bar{\Delta}_s\bar{\Delta}_o + \bar{s}^2M\bar{\beta}_o = 0, \tag{11}$$

we can solve for the values of $\bar{s}$ that satisfy this characteristic equation. For the present we consider the undamped case where $\zeta_s = \zeta_o = 0$. For this case, $\bar{\beta}_o = 1$, $\bar{\Delta}_o = \bar{s}^2 + 1$, and $\bar{\Delta}_s = \bar{s}^2 + \bar{\omega}_s^2$, so Eq. (11) can be written as

$$\bar{s}^4 + (1 + \bar{\omega}_s^2 + M)\bar{s}^2 + \bar{\omega}_s^2 = 0. \tag{12}$$

Substituting $z = -\bar{s}^2 = \bar{\omega}^2$,

$$z^2 - (1 + \bar{\omega}_s^2 + M)z + \bar{\omega}_s^2 = 0, \tag{13}$$

$$z = \frac{(1 + \bar{\omega}_s^2 + M)}{2} \pm \left(\frac{(1 + \bar{\omega}_s^2 + M)^2}{4} - \bar{\omega}_s^2\right)^{1/2}. \tag{14}$$

Thus,

$$\bar{\omega}_{1,2} = \left(\frac{(1 + \bar{\omega}_s^2 + M)}{2} \pm \left(\frac{(1 + \bar{\omega}_s^2 + M)^2}{4} - \bar{\omega}_s^2\right)^{1/2}\right)^{1/2}. \tag{15}$$

Equation (15) defines the two natural frequencies of the combined 2-degree of freedom system. One of these will always be less than the natural frequency

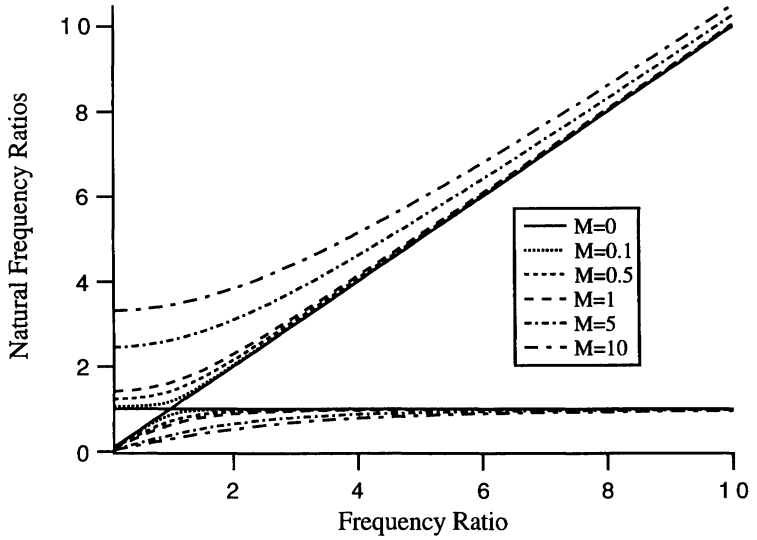

FIGURE 5 Natural frequency ratios as a function of frequency ratio for various mass ratios.

of the test object, ω_o, because

$$\bar{\omega}_1 = \left[\frac{(1+\bar{\omega}_s^2+M)}{2} - \left(\frac{(1+\bar{\omega}_s^2+M)^2}{4} - \bar{\omega}_s^2\right)^{1/2}\right]^{1/2} \leqslant 1, \quad (16)$$

while the other will always be greater than ω_o and greater than ω_s, because

$$1 \leqslant \bar{\omega}_2 = \left[\frac{(1+\bar{\omega}_s^2+M)}{2} + \left(\frac{(1+\bar{\omega}_s^2+M)^2}{4} - \bar{\omega}_s^2\right)^{1/2}\right]^{1/2} \quad (17a)$$

and

$$\omega_s \leqslant \bar{\omega}_2 = \left[\frac{(1+\bar{\omega}_s^2+M)}{2} + \left(\frac{(1+\bar{\omega}_s^2+M)^2}{4} - \bar{\omega}_s^2\right)^{1/2}\right]^{1/2}. \quad (17b)$$

The natural frequency ratios $\bar{\omega}_1$ and $\bar{\omega}_2$ are plotted in Fig. 5 as functions of the frequency ratio $\bar{\omega}_s$ for various mass ratios M. Although $M = 0$ does not represent a realistic case, because it would require a massless test object, it represents a limiting case and defines asymptotes that are approached in the other cases as $\bar{\omega}_s$ increases. As M increases, these asymptotes are approached only for larger values of $\bar{\omega}_s$. For larger values of $\bar{\omega}_s$, the natural frequency ratio represented by Eq. (16) approaches unity while the natural frequency ratio represented by Eq. (17) approaches $\bar{\omega}_s$, indicating that the two oscillators become dynamically uncoupled and the system natural frequencies become those of the original natural frequencies of the two oscillators before they were connected to each other. The difference between each of the coupled system natural frequencies and their respective original values (ω_o or ω_s, respectively) before coupling is plotted in Fig. 6. From Fig. 6, for example, we see that for $M = 1$ the differences between the coupled and uncoupled natural frequencies is near zero for $\omega_s > 8$, indicating near uncoupling of the resonances by frequency separation.

If the compliance of supporting structure s is negligible then $v_i = v_g$ so the velocity at port g is transferred directly to port i, and using Eqs. (1) the following transfer functions are defined

$$\frac{v_i}{v_g} = 1, \quad (18)$$

$$f_i = \frac{\beta_o}{\Delta_o} f_o + \frac{m_o \beta_o s}{\Delta_o} v_g, \quad (19)$$

$$v_o = -\frac{s}{m_o \Delta_o} f_o + \frac{\beta_o}{\Delta_o} v_g. \quad (20)$$

Converting Eqs. (18)–(20) to nondimensional frequency form as before,

$$\bar{v}_i = \bar{v}_g, \quad (21)$$

$$\bar{f}_i = \frac{\bar{\beta}_o}{\bar{\Delta}_o} \bar{f}_o + \frac{j\bar{\omega}\bar{\beta}_o}{\bar{\Delta}_o} \bar{v}_g, \quad (22)$$

$$\bar{v}_o = \frac{-j\bar{\omega}}{\bar{\Delta}_o} \bar{f}_o + \frac{\bar{\beta}_o}{\bar{\Delta}_o} \bar{v}_g. \quad (23)$$

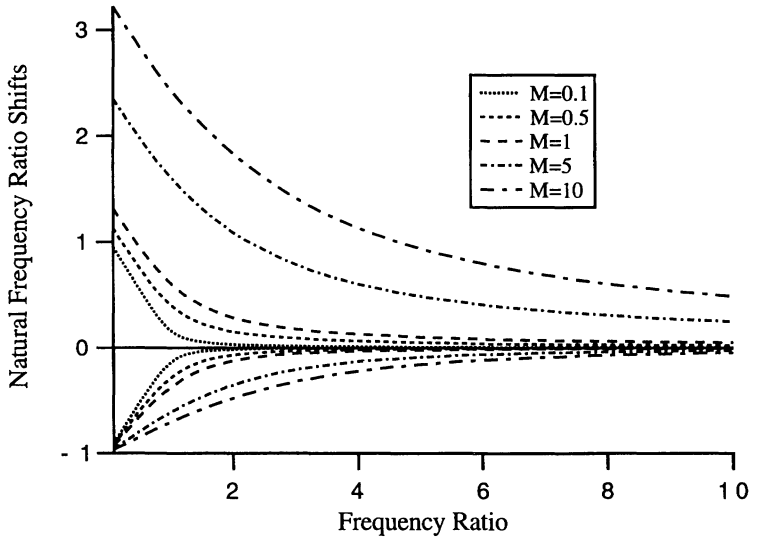

FIGURE 6 Natural frequency ratio shift as a function of frequency ratio for various mass ratios.

The denominators then indicate resonance only at the natural frequency of the test object, that is, there is no coupling between the two oscillators. Notice that when $\bar{\omega}_s \gg 1$ and $\bar{\omega} \ll \bar{\omega}_s$, then $\bar{\omega}^2 M \bar{\beta}_o \ll \bar{\beta}_s \approx \bar{\Delta}_s$ and Eqs. (8)–(10) reduce to Eqs. (21)–(23), again illustrating the uncoupling that occurs as $\bar{\omega}_s$ gets large. Another way to look at frequency uncoupling is to compare the response functions Eqs. (8)–(10), versus Eqs. (21)–(23) in the frequency range of interest indicated by Eqs. (8)–(10).

Let us now use the 2-degree of freedom model above to consider some practical problems in shaker test design.

INFINITE SERVICE IMPEDANCE AND LOW SHAKER IMPEDANCE

Suppose again the test object and shaker each can be modeled by a single degree of freedom within the frequency range of interest. First we see that if the supporting structure in service and in testing present infinite impedance to the test article, then $v_i = v_g$ in Eqs. (22) and (23). And if we assume that $v_i = 0$ in service and that the object is excited in service by the force f_o and in testing by a velocity v_i such that the relative velocity $(v_o - v_i)$ is the same as that in service, then we have the same circumstance discussed under the single degree of freedom model above, wherein f_i in the test is representative of f_i during service.

If, on the other hand, the shaker cannot produce the desired input v_i, but rather produces the input $v_g \neq v_i$ because the dynamics of the shaker are not successfully uncoupled from the dynamics if the test object, then Eqs. (8)–(10) can be used to determine the response created by the input v_g. The dynamics of the shaker will change the response of the test object such that the frequency response function relating $\bar{v}_i$ and $\bar{v}_g$ in Eq. (8) will typically exhibit two resonances that appear on either side of the natural frequency of the test object, with an antiresonance between.

One of the objectives of a shaker controller is to compensate for the shaker dynamics. This is typically done by feeding back the shaker motion, v_i, in the above model, Eqs. (8)–(10), and adjusting the input v_g to make v_i equal to the desired motion, in effect increasing the shaker natural frequency so $\bar{\omega}_s \gg 1$. Thus, after feedback compensation, $v_i = v_g$, at least within the ability of the controller to maintain that objective. Physical limitations make this impossible for all frequencies without infinite power and infinite strength shaker components, but a well designed shaker will be capable of maintaining the shaker motion, v_i, within the frequency range over which it is to be used. If the controller can extend the bandwidth of the shaker to make the lowest natural frequency of the controlled shaker high enough to uncouple its dynamics and make the shaker impedance relatively high over the frequency range of interest, then Eqs. (21)–(23) effectively model the test dynamics.

INFINITE SHAKER IMPEDANCE AND LOW SERVICE IMPEDANCE

We considered the case where the shaker impedance is not effectively infinite over the frequency range of

the test and have noted the effect of dynamic interactions of the test object with the shaker. Another case that can be considered using the same model is that in which the shaker impedance is effectively infinite but the impedance of the supporting structure in service is not infinite, allowing dynamic interactions in service that are not the same as in testing. Figures 5 and 6 can be used to estimate the degree of coupling for this case as well by appropriate determination of the important frequency and mass ratios.

USING OUTPUT AUTOSPECTRA TO CONTROL TESTS

We turn now to represent the cases considered above in terms of autospectra and calculate $\overline{F}_i^t$ relative to $\overline{F}_i^s$ as functions of frequency for various cases of damping and mass and frequency ratios. First is the case in which the test object sees infinite impedance at port i from a supporting structure both in service and in testing as modeled by Eqs. (21)–(23). Substituting $\bar{v}_i$ from Eq. (21) into Eqs. (22) and (23),

$$\bar{v}_o = \frac{-j\bar{\omega}}{\bar{\Delta}_o}\bar{f}_o + \frac{\bar{\beta}_o}{\bar{\Delta}_o}\bar{v}_i, \tag{24}$$

$$\bar{f}_i = \frac{\bar{\beta}_o}{\bar{\Delta}_o}\bar{f}_o + \frac{-j\bar{\omega}\bar{\beta}_o}{\bar{\Delta}_o}\bar{v}_i. \tag{25}$$

Again assuming that excitation during service comes from $\bar{f}_o$ while the excitation during the shaker test comes from $\bar{v}_i$, and defining the input autospectrum during service as $\overline{F}_o$, we determine the output autospectra for $\bar{v}_o$ and $\bar{f}_i$ during service to be, respectively,

$$\overline{V}_o^s = \left(\frac{-j\bar{\omega}}{\bar{\Delta}_o}\right)\left(\frac{-j\bar{\omega}}{\bar{\Delta}_o}\right)^*\overline{F}_o = \frac{\bar{\omega}^2}{\bar{\Delta}_o\bar{\Delta}_o^*}\overline{F}_o, \tag{26}$$

$$\overline{F}_i^s = \frac{\bar{\beta}_o\bar{\beta}_o^*}{\bar{\Delta}_o\bar{\Delta}_o^*}\overline{F}_o. \tag{27}$$

Letting $f_o = 0$ and input excitation be v_i, in testing as before, the output spectra during testing are found as

$$\overline{V}_o^t = \frac{\bar{\beta}_o\bar{\beta}_o^*}{\bar{\Delta}_o\bar{\Delta}_o^*}\overline{V}_i, \tag{28}$$

$$\overline{F}_i^t = \left(\frac{-j\bar{\omega}\bar{\beta}_o}{\bar{\Delta}_o}\right)\left(\frac{-j\bar{\omega}\bar{\beta}_o}{\bar{\Delta}_o}\right)^*\overline{V}_i = \frac{\bar{\omega}^2\bar{\beta}_o\bar{\beta}_o^*}{\bar{\Delta}_o\bar{\Delta}_o^*}\overline{V}_i, \tag{29}$$

where $\overline{V}_i$ is the autospectrum of the shaker input v_i. If we control $\overline{V}_i$ during the test such that $\overline{V}_o^t = \overline{V}_0^s$, then

$$\overline{V}_i = \frac{\bar{\Delta}_o\bar{\Delta}_o^*}{\bar{\beta}_o\bar{\beta}_o^*}\overline{V}_o^t = \frac{\bar{\Delta}_o\bar{\Delta}_o^*}{\bar{\beta}_o\bar{\beta}_o^*}\frac{\bar{\omega}^2}{\bar{\Delta}_o\bar{\Delta}_o^*}\overline{F}_o = \frac{\bar{\Delta}_o\bar{\Delta}_o^*}{\bar{\beta}_o\bar{\beta}_o^*}\frac{\bar{\omega}^2}{\bar{\Delta}_o\bar{\Delta}_o^*}\frac{\bar{\Delta}_o\bar{\Delta}_o^*}{\bar{\beta}_o\bar{\beta}_o^*}\overline{F}_i^s = \frac{\bar{\omega}^2\bar{\Delta}_o\bar{\Delta}_o^*}{\bar{\beta}_o^2\bar{\beta}_o^{*2}}\overline{F}_i^s,$$

which when substituted into Eq. (29) results in

$$\overline{F}_i^t = \frac{\bar{\omega}^2\bar{\beta}_o\bar{\beta}_o^*}{\bar{\Delta}_o\bar{\Delta}_o^*}\frac{\bar{\omega}^2\bar{\Delta}_o\bar{\Delta}_o^*}{\bar{\beta}_o^2\bar{\beta}_o^{*2}}\overline{F}_i^s$$

or

$$\overline{F}_i^t = \frac{\bar{\omega}^4}{\bar{\beta}_o\bar{\beta}_o^*}\overline{F}_i^s. \tag{30}$$

Thus, if we duplicate the velocity spectrum $\overline{V}_o^t = \overline{V}_o^s$ by the test, the forces are not duplicated. Similarly, if we conduct the test by controlling v_i such that we duplicate the force in the object, f_i, then we find that the output velocity spectra will be different, having the relationship

$$\overline{V}_o^t = \frac{\bar{\beta}_o\bar{\beta}_o^*}{\bar{\omega}^4}\overline{V}_o^s = \frac{1+4\zeta_o^2\bar{\omega}^2}{\bar{\omega}^4}\overline{V}_o^s. \tag{31}$$

Therefore, creating a paricular output during testing by excitation at an input other than the one that created the particular output in service does not in general create other outputs the same as in service. For this particular single degree of freedom model, the same force spectrum is created in testing as was seen in service ($\overline{F}_i^t = \overline{F}_i^s$) when the spectrum of the relative velocity ($v_i - v_o$) created during testing is the same as in service. This, of course, does not imply that the creation of the relative motion between two points on a structure duplicates the internal forces (stresses) elsewhere in the structure.

Because the output velocities given in Eq. (31) have the same relationship as the output accelerations, the ratio of A_o^t/A_o^s given in Eq. (31) is plotted in Fig. 7. Here we see that, if we wish to match the force spectra (by matching relative velocity or acceleration spectra), the test output absolute acceleration should be higher than the service output absolute acceleration at frequencies below the natural frequency and lower at frequencies above the natural frequency.

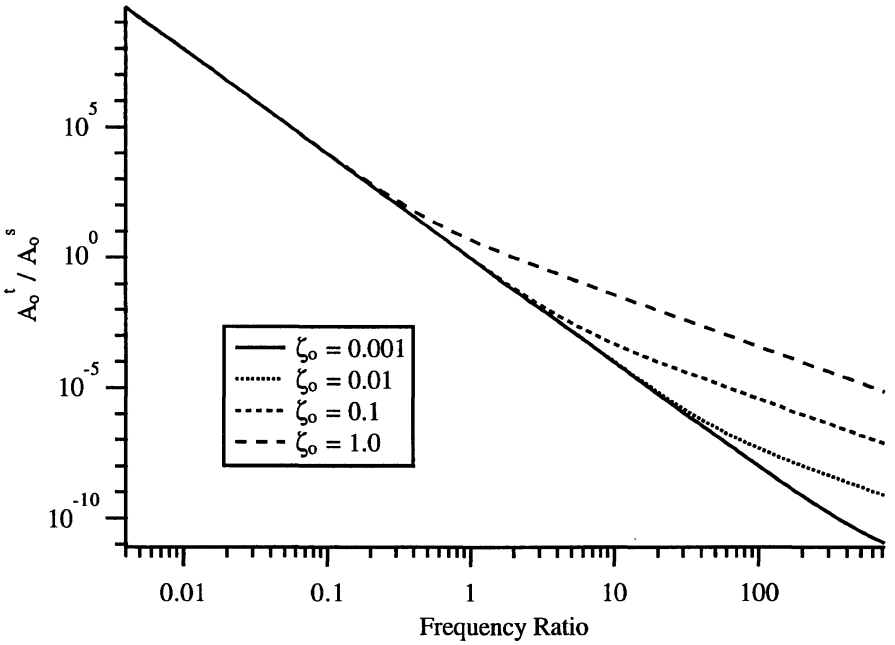

FIGURE 7 Ratio of output absolute acceleration spectra required to match relative motions or stresses.

RATIOS OF FORCE SPECTRA, INFINITE SHAKER IMPEDANCE, AND LOW SERVICE IMPEDANCE

Now suppose the test object is to be tested on an infinite impedance shaker as in the preceding case, but in service does not see infinite impedance. Assume that in service the system is fixed at port g such that $v_g = 0$, and the system is excited by the input f_o. Applying Eqs. (8)–(10) and defining for convenience the denominator as $\overline{D} = \bar{\Delta}_s\bar{\Delta}_o - \bar{\omega}^2 M\bar{\beta}_o$, we determine the output autospectrum of $\bar{v}_o$ during service as

$$\overline{V}_o^s = \frac{\bar{\omega}^2(\bar{\Delta}_s + M\bar{\beta}_o)(\bar{\Delta}_s^* + M\bar{\beta}_o^*)}{\overline{D}\,\overline{D}^*}\overline{F}_o \tag{32}$$

and the output autospectrum of $\bar{f}_i$ during service as

$$\overline{F}_i^s = \frac{\bar{\beta}_o\bar{\beta}_o^*\bar{\Delta}_s\bar{\Delta}_s^*}{\overline{D}\,\overline{D}^*}\overline{F}_o. \tag{33}$$

Combining Eqs. (32) and (33),

$$\overline{F}_i^s = \frac{\bar{\beta}_o\bar{\beta}_o^*\bar{\Delta}_s\bar{\Delta}_s^*}{\overline{D}\,\overline{D}^*}\,\frac{\overline{D}\,\overline{D}^*}{\bar{\omega}^2(\bar{\Delta}_s + M\bar{\beta}_o)(\bar{\Delta}_s^* + M\bar{\beta}_o^*)}\overline{V}_o^s$$

$$= \frac{\bar{\beta}_o\bar{\beta}_o^*\bar{\Delta}_s\bar{\Delta}_s^*}{\bar{\omega}^2(\bar{\Delta}_s + M\bar{\beta}_o)(\bar{\Delta}_s^* + M\bar{\beta}_o^*)}\overline{V}_o^s$$

or

$$\overline{F}_i^s = \frac{\bar{\beta}_o\bar{\beta}_o^*\bar{\Delta}_s\bar{\Delta}_s^*}{\bar{\omega}^2(\bar{\Delta}_s\bar{\Delta}_s^* + M^2\bar{\beta}_o\bar{\beta}_o^* + M\{\bar{\beta}_o\bar{\Delta}_s^* + \bar{\beta}_o^*\bar{\Delta}_s\})} \times \overline{V}_o^s. \tag{34}$$

If the test object is now removed from the service structure and mounted upon a shaker table with infinite impedance, then Eqs. (24) and (25) apply, which when combined yield

$$\overline{F}_i^t = \bar{\omega}^2\overline{V}_o^t. \tag{35}$$

Thus,

$$\frac{\overline{F}_i^t}{\overline{F}_i^s} = \frac{\bar{\omega}^4(\bar{\Delta}_s\bar{\Delta}_s^* + M^2\bar{\beta}_o\bar{\beta}_o^* + M\{\bar{\beta}_o\bar{\Delta}_s^* + \bar{\beta}_o^*\bar{\Delta}_s\})}{\bar{\beta}_o\bar{\beta}_o^*\bar{\Delta}_s\bar{\Delta}_s^*} \times \frac{\overline{V}_o^t}{\overline{V}_o^s}. \tag{36}$$

Now if the test is conducted to make the spectrum of the absolute velocity v_o during testing equal to its spectrum during service, then

$$\frac{\overline{V}_o^t}{\overline{V}_o^s} = 1$$

and the ratio of the force spectra at port i is immediately seen in Eq. (36). If, on the other hand, the test is

conducted so that the spectrum of the relative velocity $(v_o - v_i)$ during testing matches the spectrum of the relative velocity $(v_o - v_g)$ during service, the input spectra will be chosen such that

$$\frac{\overline{V}_o^t}{\overline{V}_o^s} = \frac{\bar{\beta}_o \bar{\beta}_o^*}{\bar{\omega}^4},$$

so that

$$\frac{\overline{F}_i^t}{\overline{F}_i^s} = \frac{\bar{\Delta}_s \bar{\Delta}_s^* + M^2 \bar{\beta}_o \bar{\beta}_o^* + M(\bar{\beta}_o \bar{\Delta}_s^* + \bar{\beta}_o^* \bar{\Delta}_s)}{\bar{\Delta}_s \bar{\Delta}_s^*}. \tag{37}$$

In this case the internal force(s) in the test object will be different during testing than they were during service because the object was interfaced with a lower impedance structure than the high impedance of the shaker. In a frequency range where these simple models apply, we can predict the change in the spectrum of the force during testing as compared to the force in service.

Substituting into Eq. (37) the relations

$$\begin{aligned} \bar{\Delta}_s &= \bar{\omega}_s^2 - \bar{\omega}^2 + j2\zeta_s \bar{\omega}_s \bar{\omega}, \\ \bar{\beta}_s &= \bar{\omega}_s^2 + j2\zeta_s \bar{\omega}_s \bar{\omega}, \\ \bar{\beta}_o &= 1 + j2\zeta_o \bar{\omega}, \end{aligned}$$

results in

$$\frac{\overline{F}_i^t}{\overline{F}_i^s} = 1 + \frac{M^2(1 + 4\zeta_o^2 \bar{\omega}^2) + 2M(\bar{\omega}_s^2 - \bar{\omega}^2\{1 - 4\zeta_o \zeta_s \bar{\omega}_s\})}{(\bar{\omega}_s^2 - \bar{\omega}^2)^2 + 4\zeta_s^2 \bar{\omega}_s^2 \bar{\omega}^2}. \tag{38}$$

By plotting $\overline{F}_i^t / \overline{F}_i^s$ as a function of $\bar{\omega}$ for various values of $\bar{\omega}_s$, M, ζ_s, and ζ_o, we can examine the effect of the changes in interface impedance upon the spectrum of the internal force.

Figure 8 shows this spectra ratio for $M = 1$, $\zeta_o = 0.1$, and $\zeta_s = 0.01$ for two different values of $\bar{\omega}_s$ ($\bar{\omega}_s = 1$ and 4). The general effect is to increase the spectrum of f_i during testing as compared to that in service below and near the natural frequency of the service structure. This leads to overtesting of the structure. Recently, force limiting at the shaker–test object interface has been proposed as a way to reduce the sharp rise in force at these frequencies. Although force limiting may reduce the amount of overtesting, it cannot totally compensate for this change in boundary conditions. A sharp peak occurs at the natural frequency of the service structure (denoted by $\bar{\omega}_s$). The overtesting at low frequencies decreases as $\bar{\omega}_s$ increases.

With Figs. 8–11, three parameters, A_{norm}, R_{rms}, and P, are determined from the data plotted in the figure. A_{norm} represents the area under the curve divided by the area that would be under the curve if its amplitude were 1 over the bandwidth plotted. In other words, it represents the ratio of the mean squared value of the internal force, f_i, during testing and the mean squared value it would have had in service. R_{rms} is the square root of A_{norm}, thus making it a ratio similar to that of root mean square forces. P is simply the peak value of the plot, as found during the plotting process. P may vary somewhat with the resolution of plotting, especially for lightly damped systems and sharp peaks, but the tabulated values were all calculated using a frequency resolution of 0.05 Hz. In any case, these parameters provide an additional quantitative measure of the errors in testing created by boundary condition changes.

Figure 9 illustrates the effect of damping in the test object. The more heavily damped the test object, the broader the frequency range and the more significant the overtesting in the frequency range near the natural frequency of the service structure.

In Fig. 10, we consider the effect of damping in the service structure. The more heavily damped the service structure, the less severe the overtesting in the frequency region near the service structural resonance. The most reliable test condition (most easily allowing reproduction of service conditions via shaker testing) occurs when the service structure is heavily damped and has a high natural frequency relative to the frequencies of interest in the test object.

Examining Fig. 11 we note that a lower mass ratio (lighter test object relative to service structure) reduces the severity of overtesting, especially at frequencies below the service structural resonance.

SUMMARY AND CONCLUSIONS

Reproducing absolute motions in testing rather than relative motions in general understresses each mode of the test object at frequencies below its natural frequency and overstresses each mode at frequencies above its natural frequency.

The dynamics of the shaker (actuators, table, etc.) interact with the dynamic properties of the test object, thus contaminating the test unless they are effectively uncoupled from the dynamics of the test object. The most effective way to provide this uncoupling is to design the shaker–controller system so that its (unloaded) natural frequencies are high relative to the

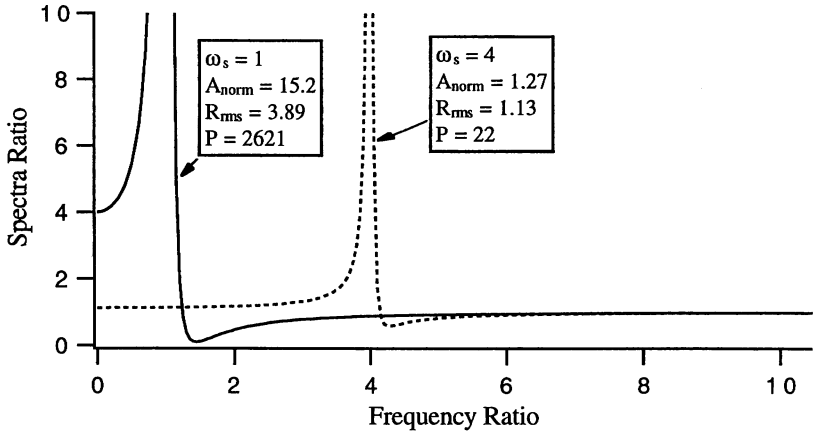

FIGURE 8 Ratio of spectra of test force to service force. $M = 1$, $\zeta_o = 0.1$, $\zeta_s = 0.01$.

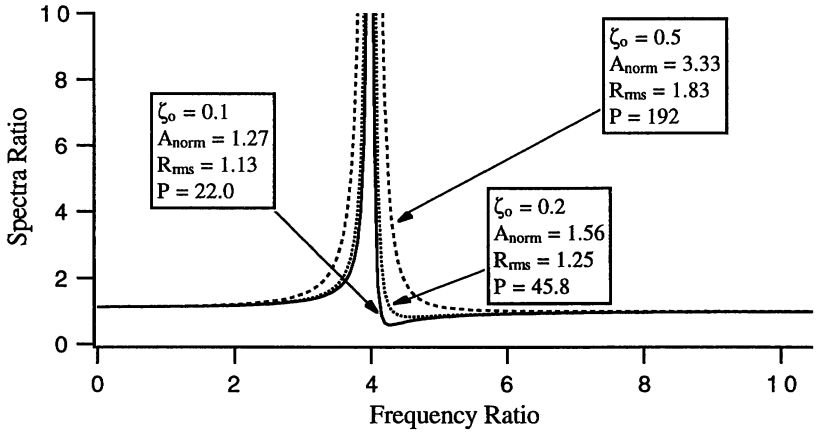

FIGURE 9 Ratio of spectra of test force to service force. $M = 1$, $\bar{\omega}_s = 4$, $\zeta_s = 0.01$.

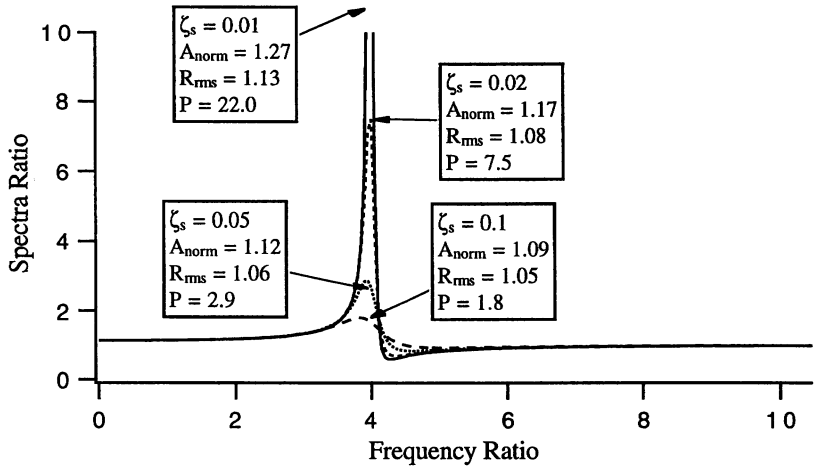

FIGURE 10 Ratio of spectra of test force to service force. $M = 1$, $\bar{\omega}_s = 4$, $\zeta_o = 0.1$.

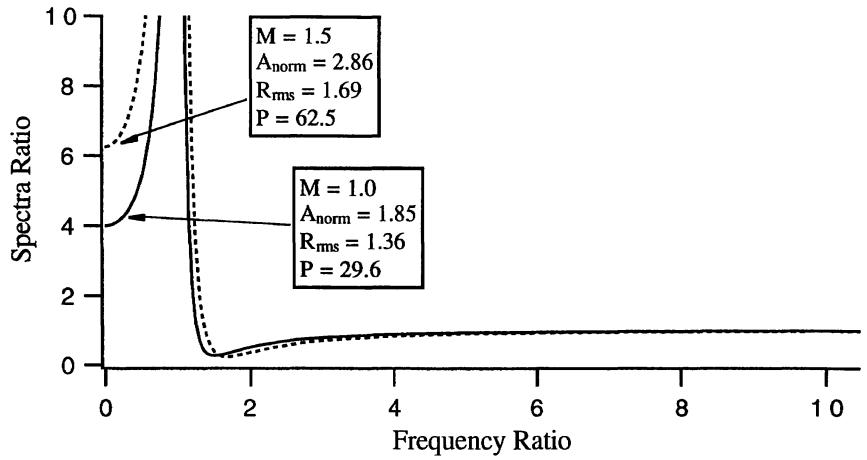

FIGURE 11 Ratio of spectra of test force to service force. $M = 1.5, \bar{\omega}_s = 1, \zeta_o = 0.1, \zeta_s = 0.1$.

frequencies over which the test(s) will be conducted. These shaker natural frequencies must be higher as the mass of the test object increases. Frequency and mass ratios are defined that can be used to quantify the degree of this dynamic coupling and determine the range over which a given shaker can be used to conduct reliable tests.

Because the shaker must have high impedance over the range of frequencies for which it will be used in order to minimize shaker–test object dynamic interactions, the impedance of the structure to which the test object is attached in service must also be high so boundary conditions in testing match those in service. When the impedance of the service structure from which the test object is attached in service is low relative to the shaker fixturing, reproduction of output spectra causes overtesting at frequencies up to the natural frequencies of the service structure. This overtest is particularly severe near the natural frequencies of the service structure. This problem is reduced for higher natural frequencies of the service structure and a smaller mass of the test object. Greater damping of the service structure reduces the severity near the natural frequencies of the service structure, whereas greater damping in the test object increases the severity of overtesting near the natural frequency of the service structure. The severity of the effects of these boundary condition changes can be characterized by frequency, mass, and damping ratios.

REFERENCES

Bausch, H. P., and Good, M., 1992, "Every Which Way But Loose—Part I," *Sound and Vibration*, Vol. 26.

Bausch, H. P., and Good, M., 1995, "Every Which Way But Loose—Part II," *Sound and Vibration*, Vol. 29.

Bonnot, P., 1986, "New Vibration Test Facility at ESTEC: The 280 kN Eletrodynamic Multishaker," *European Space Agency Journal*, Vol. 10, pp. 173–181.

Chang, K. Y., and Frydman, A. M., 1990, "Three Dmensional Test Requirement for Random Vibration Testing," *Proceedings of the Institute of Environmental Sciences.*

Fisher, D. K., and Posehn, M. R., 1977, "Digital Control System for a Multiple-Actuator Shaker," *Shock and Vibration Bulletin*, Vol. 47, pp. 79–96.

Frydman, A., 1988, "Triaxis Vibration System," Presentation to the SAE G5 Committee, Los Angeles, CA, March 9.

Greenfield, J. F., 1983, "Principles, State of the Art and Developments in Digital Random Shaker Control," *Noise and Vibration Control Worldwide*, Vol. 14, No. 5, pp. 139–142.

Hershfield, D., 1995, "A Six Degree of Freedom Hydraulic Shaker," Presentation to the Spacecraft and Launch Vehicle Dynamics Environments Technical Interchange Meeting at the Aerospace Corp., Los Angeles, CA, June 6–9.

Hobbs, G. H., and Mercado, R., 1984, "Six Degree of Freedom Vibration Stress Screening," *Journal of Environmental Sciences*, Vol. 27, No. 6, pp. 46–53.

Karnopp, D., and Rosenberg, R., 1975, *System Dynamics: A Unified Approach*, Wiley, New York.

Lehman, D., 1985, "Dual-Shaker Random Vibration Testing Control System," *Proceedings of the Institute of Environmental Sciences*, pp. 507–511.

Scharton, T. D., 1990, "Analysis of Dual Control Vibration Testing," *Proceedings of the Institute of Environmental Sciences*, pp. 140–146.

Scharton, T. D., 1991, "Dual Control Vibration Tests of Flight Hardware," *Proceedings of the Institute of Environmental Sciences.*

Scharton, T. D., 1993a, "Force Limited Vibration Testing at JPL," *Proceedings of the 14th Aerospace Testing Seminar*, Manhattan Beach, NY.

Scharton, T. D., 1993b, "Force-Limited Vibration Tests at JPL," *ITEA Journal*, September.

Smallwood, D. O., 1978, "Multiple Shaker Random Control with Cross Coupling," *Proceedings of the Institute of Environmental Sciences*, April 18–20, pp. 341–347.

Smallwood, D. O., 1982a, "Random Vibration Testing of a Single Test Item with a Multiple Input Control System," *Proceedings of the Institute of Environmental Sciences*, pp. 42–49.

Smallwood, D. O., 1982b, "Random Vibration Control System for Testing a Single Test Item with Multiple Inputs," Society of Automotive Engineers Paper 821482, pp. 4571–4577.

Smith, C. C., and Staffanson, F. L., 1996, "Frequency and Spatial Shaping of Inputs for Multi-Axis Shaker Testing," *Shock and Vibration*, Vol. 3, pp. 393–401.

Smith, S., Stroud, R. C., Hamma, G. A., and Johnson, L. J., 1980, "Digital Control Techniques for a Three-Axis Vibration Test System," Society of Automotive Engineers Paper 801233.

Stroud, R. C., and Hamma, G. A., 1988, "Multiexciter and Multiaxis Vibration Exciter Control Systems," *Sound and Vibration*, Vol. 22, No. 4, pp. 18–21, 24–28.

Yang, K.-T., and Park, Y.-S., 1993, "Joint Structural Parameter Identification Using a Subset of Frequency Response Function Measurements," *Mechanical Systems and Signal Processing*, Vol. 7, pp. 509–530.